symmetry

IMPACT FACTOR 2.2

CITESCORE 5.4

Article

Asymmetry in Galaxy Spin Directions: A Fully Reproducible Experiment Using HSC Data

Lior Shamir

Special Issue

Global and Local Scale Symmetry in Gravitation and Cosmology

Edited by

Prof. Dr. Eduardo Guendelman

MDPI

https://doi.org/10.3390/sym16101389

Article

Asymmetry in Galaxy Spin Directions: A Fully Reproducible Experiment Using HSC Data

Lior Shamir

Department of Computer Science, Kansas State University, 1701 Platt St., Manhattan, KS 66506, USA; lshamir@mtu.edu

Abstract: The asymmetry in the large-scale distribution of the directions in which spiral galaxies rotate has been observed by multiple telescopes, all showing a consistent asymmetry in the distribution of galaxy spin directions as observed from Earth. Here, galaxies with a redshift from HSC DR3 are annotated by their direction of rotation, and their distribution is analyzed. The results show that galaxies that rotate in the opposite direction relative to the Milky Way as observed from Earth are significantly more prevalent compared to galaxies that rotate in the same direction relative to the Milky Way. The asymmetry also forms a dipole axis that becomes stronger when the redshift gets higher. These results are aligned with observations from virtually all premier digital sky surveys, as well as space telescopes such as the HST and the JWST. This shows that the distribution of galaxy spin directions as observed from Earth is not symmetrical, and has a possible link to the rotational velocity of the Milky Way. This experiment provides data, code, and a full protocol that allows the results to be easily reproduced in a transparent manner. This practice is used to overcome the "reproducibility crisis" in science.

Keywords: galaxies; distances and redshifts—galaxies; spiral—cosmology; distance scale—cosmology; cosmic anisotropy—cosmology; large-scale structure of the universe

check for updates

Citation: Shamir, L. Asymmetry in Galaxy Spin Directions: A Fully Reproducible Experiment Using HSC Data. *Symmetry* **2024**, *16*, 1389. https://doi.org/10.3390/sym16101389

Academic Editor: Vasilis K. Oikonomou

Received: 19 September 2024
Revised: 15 October 2024
Accepted: 16 October 2024
Published: 18 October 2024

1. Introduction

The distribution of the directions of rotation of spiral galaxies has been a topic of study for several decades, often with conflicting results. While the null hypothesis is that the number of galaxies rotating in one direction is the same as the number of galaxies rotating in the opposite direction, multiple studies starting as early as the 1980s have provided consistent results showing that the distribution of galaxies in the sky does not necessarily satisfy the null hypothesis. At the same time, other studies have argued that the null hypothesis agrees with observations.

Early observations were based on a relatively small number of galaxies classified manually by the shape of the galaxy arms, showing asymmetry between the number of spiral galaxies that rotate clockwise and the number of spiral galaxies that rotate counterclockwise with a confidence of 92% [1]. The deployment of robotic telescopes allowed for studying far more galaxies, using autonomous digital sky surveys such as the Sloan Digital Sky Survey (SDSS) [2–7].

Other digital sky surveys also showed asymmetry between the number of galaxies rotating clockwise and the number of galaxies rotating counetrclockwise. These experiments include DECam [8], Pan-STARRS [5], the Dark Energy Survey [9,10], and the DESI Legacy Survey [11]. These sky surveys cover both the Northern and Southern Hemispheres, and show that the asymmetry in the distribution of galaxy spin directions forms a cosmological-scale dipole axis [5,8,9,11]. Other experiments were based on space telescopes such as the Hubble Space Telescope [12], and the James Webb Space Telescope [13]. The James Webb Space Telescope deep field image acquired inside the field of the HST's Ultra Deep Field allows us to notice the asymmetry by simple manual inspection [13].

The asymmetry and the large-scale axis exhibited by it might be related to anomalies in the large-scale structure of the Universe, and can agree with other theories such as rotating Universe [14–20], or black hole cosmology [21–28]. On the other hand, the locations of the most likely axes in all experiments are within close proximity to the Galactic pole [29]. That leads to the possibility that the dipole axis is not necessarily of cosmological origin, but could be due to differences in the brightness of the galaxies driven by their rotational velocity relative to the Galactic pole [29–32].

While numerous experiments using several different telescopes showed that the distribution of galaxy spin directions is not fully random, other studies showed no statistically significant asymmetry [33–37]. These claims were addressed in previous studies that aimed at the reproduction and careful analysis of these experiments to understand the reasons for why they provided random distributions [11,13,38–40].

This paper shows an experiment using galaxies with redshifts imaged by the Hyper Suprime-Cam (HSC). The redshift and the powerful imaging power of the HSC allows us to analyze galaxies with a higher redshift compared to other Earth-based telescopes, and to therefore better profile the change in the asymmetry in response to the redshift of the galaxies. The code and data are provided, allowing researchers to easily reproduce the experiment and inspect the consistency of the data. This makes the experiment different from most previous studies of this question. This paper also discusses the question of the distribution of galaxy spin directions in light of the current "reproducibility crisis" in science.

2. Data

The data used in this experiment include galaxies with a redshift imaged by the HSC and included in the HSC third data release (DR3). The HSC uses the powerful 8.2 m Subaru telescope, providing it with imaging power stronger than other Earth-based digital sky surveys such as SDSS, Pan-STARRS, or DES. The HSC can therefore provide images with high amounts of details of the galaxy shapes, allowing us to observe the arms of galaxies at higher redshift ranges compared to any other Earth-based digital sky survey. The downside of the HSC is that its footprint size is smaller compared to some other Earth-based digital sky surveys.

The dataset used in this experiment is the same dataset used in [41], and the full details regarding the preparation of the dataset are described in that paper. In summary, the initial set of galaxies included all galaxies with a redshift in the HSC DR3. Because the HSC is not a spectroscopic survey, the redshifts of the galaxies are taken from SDSS DR17. This included 101,415 galaxies with redshifts of $0 < z < 0.3$.

After the images of all galaxies were downloaded, the galaxies were annotated by their direction of rotation. Annotating 10^5 galaxies is definitely a labor-intensive task that is largely impractical to do manually. More importantly, manual annotation is subjected to cognitive biases that are very difficult to quantify and control. Therefore, the entire process of annotating the galaxies was performed in a fully automatic manner, and without any human intervention except for inspection of the annotation. The spin directions of galaxies were annotated by the *Ganalyzer* algorithm [42,43] as described in [8–11,32,41,44]. The *Ganalyzer* algorithm and the way it was used are described in a large number of previous papers [8–11,32,41,42,44].

In summary, the *Ganalyzer* first converts each galaxy image into its radial intensity plot transformation. Then, for each radial distance from the center of the galaxy, it applies peak detection to identify bright pixels. Because arm pixels are brighter than background pixels, the bright pixels are expected to be on the galaxy arms. If the polar angle of these bright pixels changes with the radial distance, it means that the arm is curved, and the direction of the curve can identify the direction of the rotation of the galaxy. This is found by applying a linear regression to the bright pixels on the radial intensity plot, and the sign of the regression coefficient determines the direction of the arm curve. The full details with thorough experimental results are available at [8–11,32,41,42,44].

The *Ganalyzer* is a fully symmetric algorithm [42], and its simple and "mechanical" nature allows us to understand and control the way it works. The explainable nature of the *Ganalyzer* makes it different from machine learning and deep neural network solutions. The complex nature of these algorithms makes them difficult to fully profile, leading to unexpected biases [45,46].

As described with the experimental results in [8–11,44], the *Ganalyzer* annotates the sign of the direction of the rotation of galaxies (clockwise or counterclockwise) with virtually no errors. That is, it would very rarely classify a galaxy that rotates clockwise as a galaxy that rotates counterclockwise. At the same time, the algorithm also rejects galaxies that the algorithm cannot determine the direction of rotation for. As described in [42], if the absolute value of the coefficient of the linear regression is smaller than 0.35, the slope is determined to be too weak to identify the direction of rotation of the galaxy. In that case, the galaxy is ignored and not used in the analysis. In the HSC DR3 image data, ∼86% of the galaxies were ignored, which means that these galaxies were elliptical, irregular, or that their shape did not allow the algorithm to identify their direction of rotation.

When the annotation of the galaxies was completed, it provided a very clean dataset of 13,477 galaxies [41]. The dataset can be downloaded at https://people.cs.ksu.edu/~lshamir/data/asymmetry_hsc/ (accessed on 16 October 2024). An inspection of 100 galaxies shows that the annotations of all of these galaxies are in agreement with the annotation of the human eye, and in all cases, the annotation is clear and correct. No in-between cases were identified, as such cases are rejected by the algorithm and these galaxies are not assigned an annotation. The 100 galaxies were selected such that 50 galaxies had a redshift lower than 0.1 and 50 had a redshift higher than 0.1, to ensure that the correctness of the annotation does not degrade when the galaxies have higher redshifts. The annotation was repeated after mirroring all galaxy images to ensure that the analysis is symmetrical, and that mirroring the galaxy images does not change the annotation. In cases with galaxies with unique shapes or features that can confuse the algorithm, it is expected that such galaxies will be distributed evenly between galaxies that rotate in both directions.

Figure 1 shows the distribution of the redshifts of the galaxies. Naturally, the number of annotated galaxies decreases as the redshift range becomes higher, as at higher redshifts, the number of galaxies whose shape can be identified gets smaller. Figure 2 shows the RA distribution of the galaxies in the dataset, which is driven by the footprint of the HSC DR3. Since the HSC DR3 does not cover all RA ranges, some RA ranges do not have galaxies in them. The RA ranges of $[45°, 120°]$ and $[255°, 330°]$ are not within the HSC DR3 footprint, and therefore contain no galaxies. Since the footprint does not have galaxies in some large parts of the sky, the analysis requires a method that fits the entire set of galaxies into a statistical model, as will be explained in Section 3.

Figure 1. The redshift distribution of the galaxies. Since galaxies at higher redshift ranges tend to be smaller and dimmer, the number of annotated galaxies declines as the redshift range grows higher.

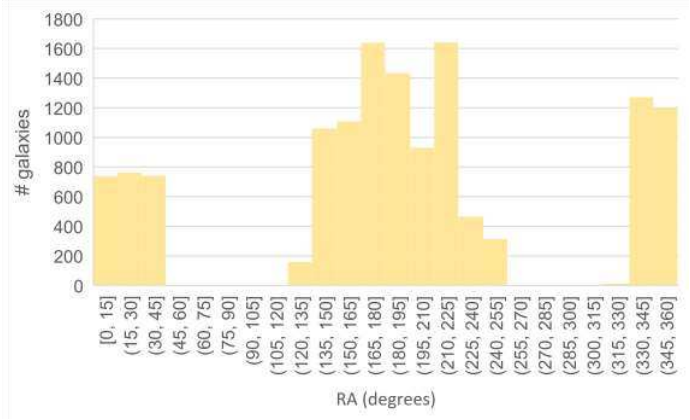

Figure 2. RA distribution of the galaxies. The distribution is driven by the footprint of the HSC DR3, and therefore some RA ranges do not contain galaxies.

Figure 3 shows the distribution of the exponential magnitude of the galaxies in the *r* band. As the graph shows, the vast majority of the galaxies have an r magnitude between 16 to 18, with very rare cases of galaxies dimmer than 18. The dataset also does not contain galaxies brighter than 13.

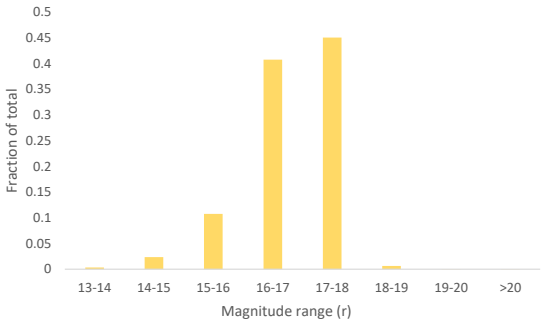

Figure 3. The magnitude distribution of the galaxies. The magnitude is the exponential magnitude of the *r* band. The vast majority of the galaxies have an exponential magnitude of 16–18.

3. Results

The first experiment was to test whether the distribution of galaxy spin directions is different in the two ends of the Galactic pole. Due to the Doppler shift effect, galaxies that rotate in the opposite direction relative to the Galactic pole are expected to be slightly brighter compared to galaxies that rotate in the same direction relative to the Galactic pole [29]. With the rotational velocity of the Milky Way of $\sim$220 km $\cdot$ s^{-1}, the expected magnitude difference is $\sim$0.006 [29]. Empirical experiments have indeed shown that the average magnitude of galaxies that rotate in the same direction relative to the Milky Way is different from the average magnitude of galaxies that rotate in the opposite direction. This was observed with data from SDSS, Pan-STARRS [31], the Hubble Space Telescope [30], and the DESI Legacy Survey [29].

Since galaxies that rotate in the opposite direction relative to the Milky Way are expected to be brighter than galaxies that rotate in the same direction relative to the Milky Way, galaxies that rotate in the same direction relative to the Milky Way are expected to be more prevalent to an Earth-based observation compared to galaxies that rotate in the same direction relative to the Milky Way. Therefore, more galaxies that rotate clockwise are expected to be observed around the Southern Galactic pole, and more galaxies rotating counterclockwise are expected to be observed at the Northern end of the Galactic pole. For instance, JWST deep field images acquired in close proximity to the Galactic pole showed that the number of galaxies that rotate in the opposite direction relative to the Milky Way is higher than the number of galaxies that rotate in the same direction relative to the Milky Way [13].

The HSC DR3 does not cover the Southern Galactic pole nor the Northern Galactic pole. But, it can be expected that the populations of galaxies that are closer to one of the ends of the Galactic poles will exhibit such asymmetry. This means that in the population of galaxies closer to the Northern Galactic pole, galaxies rotating counterclockwise will be brighter, and therefore an excessive number of counterclockwise galaxies will be observed. In the population of galaxies in the Southern end of the Galactic pole, an excessive number of clockwise galaxies is expected.

Table 1 shows the number of galaxies rotating in the same direction relative to the Milky Way and in the opposite direction relative to the Milky Way around the Northern and Southern ends of the Galactic pole. As the table shows, at both ends of the Galactic pole there are more galaxies that rotate in the opposite direction relative to the Milky Way observed from Earth. As mentioned above, this is not necessarily because galaxies that rotate in the opposite direction relative to the Milky Way are more prevalent in the Universe, but because these galaxies might be slightly brighter due to their rotational velocity relative to the rotational velocity of the Earth within the Milky Way galaxy.

Table 1. The number of spiral galaxies that rotate in the same direction relative to the Milky Way and in the opposite direction relative to the Milky Way. The p values are the binomial distribution probability to have such a distribution by chance when assuming that the probability of a galaxy rotating in a certain direction is 0.5.

Pole	# MW	# OMW	$\frac{OMW-MW}{OMW+MW}$	p Value
North	4317	4436	0.014	0.103
South	2313	2411	0.021	0.085
All	6630	6847	0.016	0.031

As the table shows, when using all galaxies in the dataset, the probability to have such a distribution by mere chance is $p \simeq 0.031$. The fact that in both ends of the Galactic pole more observed galaxies rotate in the opposite direction relative to the Milky Way shows the consistency of the asymmetry, but it also shows that it is not a feature of asymmetry in the galaxy annotation algorithm. Galaxies that rotate in the same direction relative to the Milky Way would seem to rotate counterclockwise in the Southern pole, but clockwise in the Northern Galactic pole. If the algorithm had some unknown bias towards a certain direction, that would have led to there being more galaxies that rotate in the same direction in one end of the Galactic pole, and a higher number of galaxies that rotate in the opposite direction relative to the Milky Way at the opposite end of the Galactic pole. As mentioned in Section 2, the annotation is fully symmetrical, and was tested by mirroring the images in this experiment, as well as in numerous previous experiments [4,5,7–9,11–13].

The separation of the population of galaxies that are closer to the Northern Galactic pole and galaxies that are closer to the Southern Galactic pole provides a very simple experiment that is easy to analyze and reproduce from the data. The statistical inference is also straightforward, and based on simple binomial distribution.

The higher number of galaxies that rotate in the opposite direction relative to the Milky Way is aligned with previous studies. For instance, when using the "superclean" annotations of *Galaxy Zoo 1* [34] that were also mirrored to offset for human bias, the asymmetry was 2.1% when mirroring galaxy images annotated as counterclockwise, and 1.5% when mirroring galaxy images annotated as clockwise. This is based on the values in Table 2 in [34], as explained in [11,13,38,47]. The magnitude and direction of the asymmetry agree with other datasets of SDSS galaxies with spectra, showing a difference of ∼1.1% [5]. The footprint of SDSS galaxies with spectra is such that most galaxies are around the Northern Galactic pole, leading to the asymmetry when using the entire population of galaxies in that footprint [38].

Another experiment aimed at identifying whether the asymmetry in the distribution of galaxy spin directions exhibits a cosmological-scale dipole axis. It was based on the same

analysis done in [4,5,8,9,11,12], and analyzed this thoroughly with extensive tests as in [7]. In summary, all possible integer combinations of (α, δ) are fitted to a cosine dependence with the directions of rotations of the galaxies. This is done by using χ^2 statistics shown in Equation (1), such that the χ^2 of the observed directions of rotation of the galaxies is compared to the χ^2 when assigning the galaxies with random spin directions. ϕ_i is the angular distance between (α, δ) and galaxy i, and d is the direction of rotation of the galaxy, where 1 means clockwise and -1 means counterclockwise.

$$\chi^2_{(\alpha,\delta)} = \Sigma_i \left| \frac{(d_i \cdot |\cos(\phi_i)| - \cos(\phi_i))^2}{\cos(\phi_i)} \right| \quad (1)$$

The $\chi^{2^{\alpha,\delta}}_{real}$ is computed with the observed directions of the rotations of the galaxies. The χ^2 when using the random directions of rotations is computed 1000 times for each integer (α, δ) combination, and the $\chi^{2^{\alpha,\delta}}_{random}$ is the mean $\overline{\chi^{2_{\alpha,\delta}}}$ of the 1000 runs where each run has a different set of random directions. The standard deviation $\sigma(\chi^2_{\alpha,\delta})$ is also computed using the 1000 runs. The (α, δ) that provides the highest $\frac{\chi^2_{real} - \chi^2_{random}}{\sigma(\chi^2_{\alpha,\delta})}$ is the most likely dipole axis formed by the distribution of the galaxy spin directions. The analysis is explained in full detail in [4,5,7–9,11,12]. χ^2 statistics assume the normal distribution of the galaxy spin directions, which is satisfied under the assumption that the sign of the galaxy spin direction and the inclinations of the galaxies are expected to be random.

Figure 4 shows the $\frac{\chi^2_{real} - \chi^2_{random}}{\sigma(\chi^2_{\alpha,\delta})}$ for all possible (α, δ) integer combinations. THe code and data to reproduce the experiment are available at https://people.cs.ksu.edu/~lshamir/data/asymmetry_hsc (accessed on 15 October 2024).

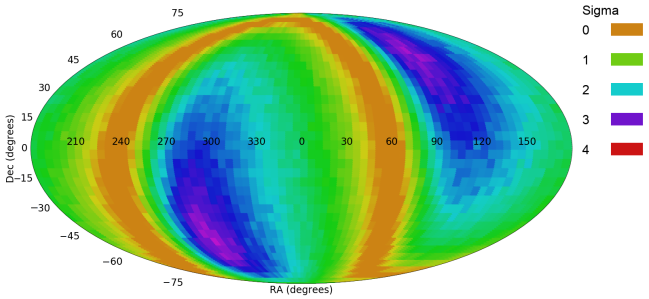

Figure 4. The χ^2 significance of a dipole axis to be formed by the distribution of galaxy spin directions in different parts of the sky.

The most likely dipole axis is at $(\alpha = 94^\circ, \delta = 52^\circ)$, with a statistical significance of 3.3σ. The 1σ error range of the location is $(39^\circ, 196^\circ)$ for the RA and $(-10^\circ, 81^\circ)$ for the declination. The HSC footprint that also overlaps with SDSS for the spectra is relatively small, at approximately 416 degree^2 [48]. The analysis identifies the best fit of a dipole axis by fitting all galaxies into a dipole axis alignment. Therefore, it is not affected by under-populated parts of the sky that can skew the location of the most likely axis. But, a smaller footprint also makes the location of the most likely dipole axis less accurate compared to previous studies that used far larger footprints.

While the relatively small footprint does not allow us to identify the dipole axis with high accuracy, its location is still within the 1σ error from the Galactic pole at approximately $(\alpha = 192^\circ, \delta = 28^\circ)$. When assigning the galaxies random spin directions instead of the observed spin directions, the maximum observed statistical significance drops to 0.51. This is expected as subtracting the χ^2 of two sets of random values is not expected to generate a signal. A reproducible analysis when assigning the galaxies with random directions of rotation is also available at https://people.cs.ksu.edu/~lshamir/data/asymmetry_hsc (accessed on 15 October 2024). Figure 5 shows the probability of having a dipole axis by

chance in different parts of the sky when the galaxies are assigned with random directions of rotation.

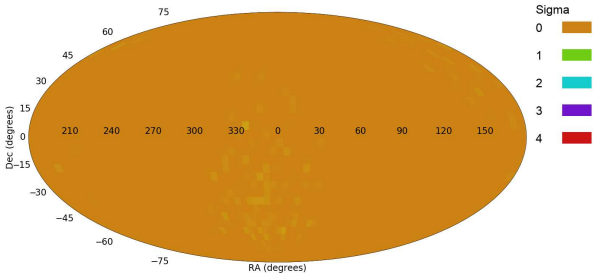

Figure 5. The χ^2 significance of a dipole axis being formed in different parts of the sky when the galaxies are assigned with random spin directions.

To test the link between the asymmetry and the redshift, the dataset can be divided into two redshift ranges: galaxies with a redshfit between 0 and 0.1, and galaxies with a reshift of 0.1 to 0.2. The two sets of galaxies have 6246, and 6214 galaxies, respectively. This makes two sets of galaxies of similar sizes. Figure 6 shows the results of the analysis using each of these two redshift ranges, with each range shown separately.

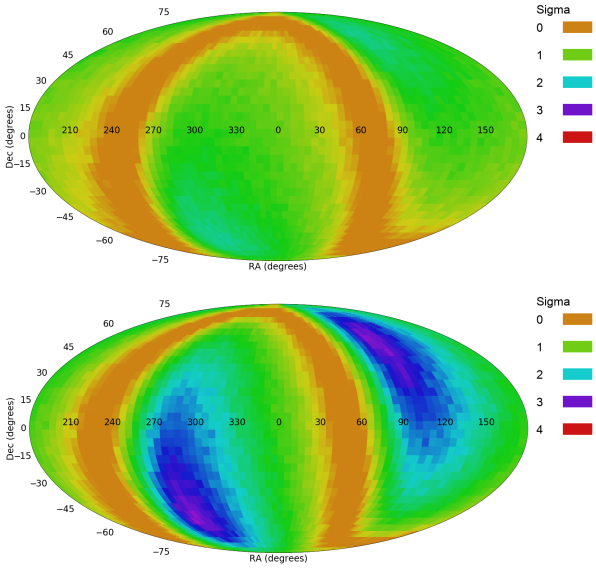

Figure 6. The χ^2 significance of a dipole axis beingformed by the distribution of galaxy spin directions in a redshift of 0 to 0.1 (**top**) and in a redshift of 0.1 to 0.2 (**bottom**). When using just galaxies with higher redshift ranges, the statistical signal is stronger. The number of galaxies used in the two experimenta is roughly the same, with 6246 and 6214 galaxies in the lower and higher redshift ranges, respectively. The two datasets to not overlap, and no galaxy was used in both experiments.

When the redshift of the galaxies is $z < 0.1$, the statistical strength of the axis is 1.79σ, peaking at $(\alpha = 114^\circ, \delta = 62)$. When the redshift range is $0.1 < z < 0.2$, the statistical strength of the dipole increases to 3.1σ, peaking at $(\alpha = 91^\circ, \delta = 50)$. Although the two experiments were based on two non-overlapping sets of galaxies, the locations of the most likely axes are close to each other, and well within the 1σ error of the dipole axis shown in Figure 4. The stronger signal when the galaxies have a higher redshift is in agreement with previous observations using other telescopes, all of which show that the magnitude of the asymmetry increases as the redshift gets higher [5,10]. When using high-redshift galaxies imaged by the JWST, the difference between the number of galaxies rotating in the same direction relative to the Milky Way and the number rotating in the opposite direction relative to the Milky Way becomes extreme, and a statistically significant difference can

even be observed by the naked eye, with no need for the automatic annotation of large datasets of galaxies [13].

4. Conclusions

While the directions of the rotations of galaxies as observed from Earth are expected to be random, several experiments have suggested that the distribution is not necessarily random. These experiments are based on several different Earth-based and space-based telescopes and both the Northern and Southern Hemispheres. This paper shows the analysis of the possible non-randomness using data provided by the HSC. While the HSC has a relatively small footprint, it is deeper than that of all other existing Earth-based digital sky surveys. This allows us to profile the asymmetry in different redshift ranges.

The results show that galaxies that rotate in the same direction relative to the Milky Way galaxy as observed from Earth are less prevalent compared to galaxies that rotate in the opposite direction relative to the Milky Way. These results also show that the signal becomes stronger when the redshift of the galaxy population gets higher. Explanations can be related to anomalies of the large-scale structure of the Universe, or to the physics of galaxy rotation.

If the galaxies had alignment in their inclinations or in their directions of rotation, asymmetry in the spin directions as observed from Earth could be expected. But, since the inclination of galaxies is expected to be completely random, as well as the direction of rotation, the probability of a galaxy rotating in a certain direction as observed from Earth is the same as its probability of rotating in the opposite direction. Therefore, asymmetry in the distribution of galaxy spin directions is not expected. But, as also discussed in Section 3, such asymmetry can be driven by differences in the brightness of galaxies, as galaxies that rotate in the opposite direction relative to the Milky Way are expected to be slightly brighter than galaxies that rotate in the same direction relative to the Milky Way.

The reproduction of scientific results has been a growing challenge in all fields of science, as most results published in scientific papers have been shown to be unreproducible [49]. This "reproducibility crisis" naturally introduces a challenge for advancing science. For this reason, the results shown in this paper are fully reproducible, with code, data, and step-by-step instructions to easily reproduce the results. This allows the entire scientific community to ensure that the data used in this study are as described in the paper, and that the results shown in this paper using these data are correct. These results are also aligned with a large collection of observations that challenge the cosmological isotropy assumption [50], as well as other recent observations and tensions that challenge the standard cosmological model [50–53].

5. Discussion

Despite over a century of research, the physics of galaxy rotation is still one of the most provocative scientific phenomena, and research efforts to fully understand the nature of galaxy rotation are still being continued. The anomaly in the galaxy rotation was observed as early as the first half of the 20th century, proposing that the nature of galaxy rotation can be explained by the contention that the visible matter of the galaxy is embedded inside a much larger halo of highly dense non-luminous matter [54]. These observations were ignored for nearly five decades, possibly due to their disagreement with the standard theories of the time [55]. Currently, the most common explanation for the anomaly of the galaxy rotation curve is the presence of dark matter [56]. Another common explanation is driven by certain modifications of Newtonian dynamics [57–60], and other explanations have also been proposed [61–71].

Previous experiments provided evidence that the photometry and spectroscopy of galaxies observed from Earth are affected by the rotational velocity of these galaxies relative to the rotational velocity of the Milky Way. For instance, it has been shown that galaxies that rotate in the opposite direction relative to the Milky Way have a lower redshift than galaxies spinning in the same direction relative to the Milky Way [32,41]. The data has also shown that galaxies that rotate in the same direction as the Milky Way are dimmer

than galaxies that spin in the opposite direction relative to the Milky Way [29,30]. Like this paper, these studies are provided with data, and the results are fully reproducible. While a small difference in the brightness is expected, the observed difference in brightness is larger than expected. This could be attributed to the yet unexplained physics of galaxy rotation, although there could be other explanations related to new physics or anomalies in the large-scale structure of the Universe [29,30].

If the brightness of galaxies as observed from Earth depends on the direction of the rotation of the galaxies relative to the Milky Way galaxy, more galaxies that rotate in the opposite direction relative to the Milky Way will be more prevalent near both ends of the Galactic pole to an Earth-based observer. This is not because these galaxies are more prevalent in the Universe, but because they are brighter and therefore easier to detect from Earth. This agrees with the observation described here, showing an excessive number of galaxies that rotate in the opposite direction compared to the Milky Way.

On the other hand, large-scale alignment of the directions towards which galaxies spin has also been reported [72–82]. If the cosmological-scale alignment forms a cosmological-scale axis that is not the Galactic pole, it can be considered a feature of the large-scale structure of the Universe. In that case, such a cosmological-scale axis can be aligned with alternative cosmological theories such as spinor-driven inflation [83], the ellipsoidal universe [84–89], the rotating universe [14–20], black hole cosmology [19–26,28,90–92], the holographic universe [93–100], and others [101,102].

If the asymmetry grows as the redshift gets higher, as shown by the HSC data, it can provide an indication that the early Universe was more consistent than the present Universe, and gradually became more chaotic as reflected by the distribution of the directions towards which galaxies rotate. This can be aligned with cosmological models that are based on the contention that the Universe was born spinning, such as rotating universe [14–20] or black hole cosmology [19–26,28,90–92].

But, as described above, the results shown here can also indicate that the photometry of galaxies is affected by their rotational velocity relative to the rotational velocity of the Milky Way. In this case, the photometry has a small but consistent bias as shown in [29–31], and a similar analysis has shown a bias in the redshift [41]. A consistent bias in the redshift can be linked to the H_o tension [103–108], and possibly the tension between the size and shape of high-redshift galaxies observed with the JWST and their expected age as determined by their redshift [109]. A bias in the redshift, if such a bias indeed exists, can explain this puzzling tension.

Funding: This research was funded in part by NSF grant 2148878.

Data Availability Statement: The code, data, and step-by-step instructions to reproduce the results are available at https://people.cs.ksu.edu/~lshamir/data/asymmetry_hsc/ accessed on 15 October 2024.

Acknowledgments: I would like to thank the two knowledgeable reviewers for the insightful comments.

Conflicts of Interest: The author declares that they have no conflicts of interest.

References

1. MacGillivray, H.; Dodd, R. The anisotropy of the spatial orientations of galaxies in the local supercluster. *Astron. Astrophys.* **1985**, *145*, 269–274.
2. Longo, M.J. Detection of a Dipole in the Handedness of Spiral Galaxies with Redshifts z 0.04. *Phys. Lett. B* **2011**, *699*, 224–229. [CrossRef]
3. Shamir, L. Handedness asymmetry of spiral galaxies with z < 0.3 shows cosmic parity violation and a dipole axis. *Phys. Lett. B* **2012**, *715*, 25–29.
4. Shamir, L. Large-scale patterns of galaxy spin rotation show cosmological-scale parity violation and multipoles. *arXiv* **2019**, arXiv:1912.05429.
5. Shamir, L. Patterns of galaxy spin directions in SDSS and Pan-STARRS show parity violation and multipoles. *Astrophys. Space Sci.* **2020**, *365*, 136. [CrossRef]

6. Shamir, L. Large-scale asymmetry between clockwise and counterclockwise galaxies revisited. *Astron. Nachrichten* **2020**, *341*, 324–330. [CrossRef]
7. Shamir, L. Analysis of the alignment of non-random patterns of spin directions in populations of spiral galaxies. *Particles* **2021**, *4*, 11–28. [CrossRef]
8. Shamir, L. Large-scale asymmetry in galaxy spin directions: Evidence from the Southern hemisphere. *Publ. Astron. Soc. Aust.* **2021**, *38*, e037. [CrossRef]
9. Shamir, L. Asymmetry in galaxy spin directions—Analysis of data from DES and comparison to four other sky surveys. *Universe* **2022**, *8*, 8. [CrossRef]
10. Shamir, L. Large-scale asymmetry in galaxy spin directions: Analysis of galaxies with spectra in DES, SDSS, and DESI Legacy Survey. *Astron. Notes* **2022**, *343*, e20220010. [CrossRef]
11. Shamir, L. Analysis of spin directions of galaxies in the DESI Legacy Survey. *Mon. Not. R. Astron. Soc.* **2022**, *516*, 2281–2291. [CrossRef]
12. Shamir, L. Galaxy spin direction distribution in HST and SDSS show similar large-scale asymmetry. *Publ. Astron. Soc. Aust.* **2020**, *37*, e053. [CrossRef]
13. Shamir, L. Galaxy spin direction asymmetry in JWST deep fields. *Publ. Astron. Soc. Aust.* **2024**, *41*, e038. [CrossRef]
14. Gödel, K. An example of a new type of cosmological solutions of Einstein's field equations of gravitation. *Rev. Mod. Phys.* **1949**, *21*, 447. [CrossRef]
15. Ozsváth, I.; Schücking, E. Finite rotating universe. *Nature* **1962**, *193*, 1168–1169. [CrossRef]
16. Ozsvath, I.; Schücking, E. Approaches to Gödel's rotating universe. *Class. Quantum Gravity* **2001**, *18*, 2243. [CrossRef]
17. Sivaram, C.; Arun, K. Primordial rotation of the universe, hydrodynamics, vortices and angular momenta of celestial objects. *Open Astron.* **2012**, *5*, 7–11. [CrossRef]
18. Chechin, L. Rotation of the Universe at different cosmological epochs. *Astron. Rep.* **2016**, *60*, 535–541. [CrossRef]
19. Seshavatharam, U.; Lakshminarayana, S. An Integrated Model of a Light Speed Rotating Universe. *Int. Astron. Astrophys. Res. J.* **2020**, *2*, 74–82.
20. Campanelli, L. A conjecture on the neutrality of matter. *Found. Phys.* **2021**, *51*, 56. [CrossRef]
21. Pathria, R. The universe as a black hole. *Nature* **1972**, *240*, 298–299. [CrossRef]
22. Easson, D.A.; Brandenberger, R.H. Universe generation from black hole interiors. *J. High Energy Phys.* **2001**, *2001*, 024. [CrossRef]
23. Seshavatharam, U.; Lakshminarayana, S. Understanding Black Hole Cosmology and the Cosmic Halt. *J. Adv. Res. Astrophys. Astron.* **2014**, *1*, 1–27.
24. Popławski, N.J. Radial motion into an Einstein–Rosen bridge. *Phys. Lett. B* **2010**, *687*, 110–113. [CrossRef]
25. Tatum, E.T. Why flat space cosmology is superior to standard inflationary cosmology. *J. Mod. Phys.* **2018**, *9*, 1867–1882. [CrossRef]
26. Christillin, P. The Machian origin of linear inertial forces from our gravitationally radiating black hole Universe. *Eur. Phys. J. Plus* **2014**, *129*, 175. [CrossRef]
27. Seshavatharam, U.; Lakshminarayana, S. Light Speed Expansion and Rotation of a Primordial Black Hole Universe having Internal Acceleration. *Int. Astron. Astrophys. Res. J.* **2020**, *2*, 83–101.
28. Chakrabarty, H.; Abdujabbarov, A.; Malafarina, D.; Bambi, C. A toy model for a baby universe inside a black hole. *Eur. Phys. J. C* **2020**, *80*, 373. [CrossRef]
29. McAdam, D.; Shamir, L. Asymmetry between galaxy apparent magnitudes shows a possible tension between physical properties of galaxies and their rotational velocity. *Symmetry* **2023**, *15*, 1190. [CrossRef]
30. Shamir, L. Asymmetry between galaxies with different spin patterns: A comparison between COSMOS, SDSS, and Pan-STARRS. *Open Astron.* **2020**, *29*, 15–27. [CrossRef]
31. Shamir, L. Large-scale photometric asymmetry in galaxy spin patterns. *Publ. Astron. Soc. Aust.* **2017**, *34*, e44. [CrossRef]
32. Shamir, L. A Simple Direct Empirical Observation of Systematic Bias of the Redshift as a Distance Indicator. *Universe* **2024**, *10*, 129. [CrossRef]
33. Iye, M.; Sugai, H. A catalog of spin orientation of southern galaxies. *Astrophys. J.* **1991**, *374*, 112–116. [CrossRef]
34. Land, K.; Slosar, A.; Lintott, C.; Andreescu, D.; Bamford, S.; Murray, P.; Nichol, R.; Raddick, M.J.; Schawinski, K.; Szalay, A.; et al. Galaxy Zoo: The large-scale spin statistics of spiral galaxies in the Sloan Digital Sky Survey. *Mon. Not. R. Astron. Soc.* **2008**, *388*, 1686–1692. [CrossRef]
35. Hayes, W.B.; Davis, D.; Silva, P. On the nature and correction of the spurious S-wise spiral galaxy winding bias in Galaxy Zoo 1. *Mon. Not. R. Astron. Soc.* **2017**, *466*, 3928–3936. [CrossRef]
36. Iye, M.; Yagi, M.; Fukumoto, H. Spin Parity of Spiral Galaxies III–Dipole analysis of the distribution of SDSS spirals with 3D random walk simulation. *Astrophys. J.* **2021**, *907*, 123. [CrossRef]
37. Patel, D.; Desmond, H. No evidence for anisotropy in galaxy spin directions. *arXiv* **2024**, arXiv:2404.06617v1. [CrossRef]
38. Shamir, L. Large-scale asymmetry in the distribution of galaxy spin directions–analysis and reproduction. *Symmetry* **2023**, *15*, 1704. [CrossRef]
39. Shamir, L. Using 3D and 2D analysis for analyzing large-scale asymmetry in galaxy spin directions. *Publ. Astron. Soc. Jpn.* **2022**, *74*, 1114–1130. [CrossRef]
40. Shamir, L. Reproducible empirical evidence of cosmological-scale asymmetry in galaxy spin directions: Comment on arXiv:2404.06617. *arXiv* **2024**, arXiv:2404.13864.

41. Shamir, L. An Empirical Consistent Redshift Bias: A Possible Direct Observation of Zwicky's TL Theory. *Particles* **2024**, *7*, 703–716. [CrossRef]
42. Shamir, L. Ganalyzer: A tool for automatic galaxy image analysis. *Astrophys. J.* **2011**, *736*, 141. [CrossRef]
43. Shamir, L. Ganalyzer: A tool for automatic galaxy image analysis. *ASCL* **2011**, ascl:1105.011. [CrossRef]
44. Shamir, L. Analysis of $\sim 10^6$ spiral galaxies from four telescopes shows large-scale patterns of asymmetry in galaxy spin directions. *Adv. Astron.* **2022**, *2022*, 8462363. [CrossRef]
45. Ball, P. Is AI leading to a reproducibility crisis in science? *Nature* **2023**, *624*, 22–25. [CrossRef]
46. Dhar, S.; Shamir, L. Systematic biases when using deep neural networks for annotating large catalogs of astronomical images. *Astron. Comput.* **2022**, *38*, 100545. [CrossRef]
47. Mcadam, D.; Shamir, L. Reanalysis of the spin direction distribution of Galaxy Zoo SDSS spiral galaxies. *Adv. Astron.* **2023**, *2023*, 4114004. [CrossRef]
48. More, S.; Sugiyama, S.; Miyatake, H.; Rau, M.M.; Shirasaki, M.; Li, X.; Nishizawa, A.J.; Osato, K.; Zhang, T.; Takada, M.; et al. Hyper Suprime-Cam Year 3 results: Measurements of clustering of SDSS-BOSS galaxies, galaxy-galaxy lensing, and cosmic shear. *Phys. Rev. D* **2023**, *108*, 123520. [CrossRef]
49. Stodden, V.; Seiler, J.; Ma, Z. An empirical analysis of journal policy effectiveness for computational reproducibility. *Proc. Natl. Acad. Sci. USA* **2018**, *115*, 2584–2589. [CrossRef]
50. Aluri, P.K.; Cea, P.; Chingangbam, P.; Chu, M.C.; Clowes, R.G.; Hutsemékers, D.; Kochappan, J.P.; Krasiński, A.; Lopez, A.M.; Liu, L.; et al. Is the observable Universe consistent with the cosmological principle? *Class. Quantum Gravity* **2023**, *40*, 094001. [CrossRef]
51. Akarsu, Ö.; Colgáin, E.Ó.; Sen, A.A.; Sheikh-Jabbari, M. Λ CDM Tensions: Localising Missing Physics through Consistency Checks. *arXiv* **2024**, arXiv:2402.04767. [CrossRef]
52. Timkov, V. Actual Problems of Modern Physics, Astrophysics, and Cosmology. *IPI Lett.* **2024**, *2*, 42–75. [CrossRef]
53. Lopes, M.; Bernui, A.; Hipólito-Ricaldi, W.S.; Franco, C.; Avila, F. Dipolar Fluence distribution of statistically isotropic FERMI Gamma-Ray Bursts. *arXiv* **2024**, arXiv:2409.01480.
54. Oort, J.H. Some Problems Concerning the Structure and Dynamics of the Galactic System and the Elliptical Nebulae NGC 3115 and 4494. *Astrophys. J.* **1940**, *91*, 273. [CrossRef]
55. Rubin, V.C. One hundred years of rotating galaxies. *Publ. Astron. Soc. Pac.* **2000**, *112*, 747–750. [CrossRef]
56. Rubin, V.C. The rotation of spiral galaxies. *Science* **1983**, *220*, 1339–1344. [CrossRef]
57. Milgrom, M. A modification of the Newtonian dynamics as a possible alternative to the hidden mass hypothesis. *Astrophys. J.* **1983**, *270*, 365–370. [CrossRef]
58. Bekenstein, J.; Milgrom, M. Does the missing mass problem signal the breakdown of Newtonian gravity? *Astrophys. J.* **1984**, *286*, 7–14. [CrossRef]
59. Milgrom, M. Bimetric MOND gravity. *Phys. Rev. D* **2009**, *80*, 123536. [CrossRef]
60. Falcon, N. A large-scale heuristic modification of Newtonian gravity as an alternative approach to dark energy and dark matter. *J. Astrophys. Astron.* **2021**, *42*, 102. [CrossRef]
61. Sanders, R. Mass discrepancies in galaxies: Dark matter and alternatives. *Astron. Astrophys. Rev.* **1990**, *2*, 1–28. [CrossRef]
62. Capozziello, S.; De Laurentis, M. The dark matter problem from f (R) gravity viewpoint. *Ann. Der Phys.* **2012**, *524*, 545–578. [CrossRef]
63. Chadwick, E.A.; Hodgkinson, T.F.; McDonald, G.S. Gravitational theoretical development supporting MOND. *Phys. Rev. D* **2013**, *88*, 024036. [CrossRef]
64. Farnes, J.S. A unifying theory of dark energy and dark matter: Negative masses and matter creation within a modified ΛCDM framework. *Astron. Astrophys.* **2018**, *620*, A92. [CrossRef]
65. Rivera, P.C. An Alternative Model of Rotation Curve that Explains Anomalous Orbital Velocity, Mass Discrepancy and Structure of Some Galaxies. *Am. J. Astron. Astrophys.* **2020**, *7*, 73–79. [CrossRef]
66. Nagao, S. Galactic Evolution Showing a Constant Circulating Speed of Stars in a Galactic Disc without Requiring Dark Matter. *Rep. Adv. Phys. Sci.* **2020**, *4*, 2050004. [CrossRef]
67. Sivaram, C.; Arun, K.; Rebecca, L. MOND, MONG, MORG as alternatives to dark matter and dark energy, and consequences for cosmic structures. *J. Astrophys. Astron.* **2020**, *41*, 4. [CrossRef]
68. Blake, B.C. Relativistic Beaming of Gravity and the Missing Mass Problem. *Bull. Am. Phys. Soc.* **2021**, *2021*, B17.00002.
69. Gomel, R.; Zimmerman, T. The Effects of Inertial Forces on the Dynamics of Disk Galaxies. *Galaxies* **2021**, *9*, 34. [CrossRef]
70. Skordis, C.; Złośnik, T. New relativistic theory for modified Newtonian dynamics. *Pattern Recognit. Lett.* **2021**, *127*, 161302. [CrossRef]
71. Larin, S.A. Towards the Explanation of Flatness of Galaxies Rotation Curves. *Universe* **2022**, *8*, 632. [CrossRef]
72. Jones, B.J.; Van De Weygaert, R.; Aragón-Calvo, M.A. Fossil evidence for spin alignment of Sloan Digital Sky Survey galaxies in filaments. *Mon. Not. R. Astron. Soc.* **2010**, *408*, 897–918. [CrossRef]
73. Tempel, E.; Stoica, R.S.; Saar, E. Evidence for spin alignment of spiral and elliptical/S0 galaxies in filaments. *Mon. Not. R. Astron. Soc.* **2013**, *428*, 1827–1836. [CrossRef]
74. Tempel, E.; Libeskind, N.I. Galaxy spin alignment in filaments and sheets: Observational evidence. *Astrophys. J. Lett.* **2013**, *775*, L42. [CrossRef]

75. Codis, S.; Pichon, C.; Pogosyan, D. Spin alignments within the cosmic web: A theory of constrained tidal torques near filaments. *Mon. Not. R. Astron. Soc.* **2015**, *452*, 3369–3393. [CrossRef]
76. Pahwa, I.; Libeskind, N.I.; Tempel, E.; Hoffman, Y.; Tully, R.B.; Courtois, H.M.; Gottlöber, S.; Steinmetz, M.; Sorce, J.G. The alignment of galaxy spin with the shear field in observations. *Mon. Not. R. Astron. Soc.* **2016**, *457*, 695–703. [CrossRef]
77. Ganeshaiah Veena, P.; Cautun, M.; van de Weygaert, R.; Tempel, E.; Jones, B.J.; Rieder, S.; Frenk, C.S. The Cosmic Ballet: Spin and shape alignments of haloes in the cosmic web. *Mon. Not. R. Astron. Soc.* **2018**, *481*, 414–438. [CrossRef]
78. Ganeshaiah Veena, P.; Cautun, M.; Tempel, E.; van de Weygaert, R.; Frenk, C.S. The Cosmic Ballet II: Spin alignment of galaxies and haloes with large-scale filaments in the EAGLE simulation. *Mon. Not. R. Astron. Soc.* **2019**, *487*, 1607–1625. [CrossRef]
79. Blue Bird, J.; Davis, J.; Luber, N.; Van Gorkom, J.; Wilcots, E.; Pisano, D.; Gim, H.; Momjian, E.; Fernandez, X.; Hess, K.; et al. CHILES VI: H i and H α observations for z < 0.1 galaxies; probing H i spin alignment with filaments in the cosmic web. *Mon. Not. R. Astron. Soc.* **2020**, *492*, 153–176.
80. Welker, C.; Bland-Hawthorn, J.; Van de Sande, J.; Lagos, C.; Elahi, P.; Obreschkow, D.; Bryant, J.; Pichon, C.; Cortese, L.; Richards, S.; et al. The SAMI Galaxy Survey: First detection of a transition in spin orientation with respect to cosmic filaments in the stellar kinematics of galaxies. *Mon. Not. R. Astron. Soc.* **2020**, *491*, 2864–2884. [CrossRef]
81. Kraljic, K.; Duckworth, C.; Tojeiro, R.; Alam, S.; Bizyaev, D.; Weijmans, A.M.; Boardman, N.F.; Lane, R.R. SDSS-IV MaNGA: 3D spin alignment of spiral and S0 galaxies. *Mon. Not. R. Astron. Soc.* **2021**, *504*, 4626–4633. [CrossRef]
82. López, P.; Cautun, M.; Paz, D.; Merchán, M.; van de Weygaert, R. Deviations from tidal torque theory: Evolution of the halo spin–filament alignment. *Mon. Not. R. Astron. Soc.* **2021**, *502*, 5528–5545. [CrossRef]
83. Bohmer, C.G.; Mota, D.F. CMB anisotropies and inflation from non-standard spinors. *Phys. Lett. B* **2008**, *663*, 168–171. [CrossRef]
84. Campanelli, L.; Cea, P.; Tedesco, L. Ellipsoidal universe can solve the cosmic microwave background quadrupole problem. *Phys. Rev. Lett.* **2006**, *97*, 131302. [CrossRef]
85. Campanelli, L.; Cea, P.; Tedesco, L. Cosmic microwave background quadrupole and ellipsoidal universe. *Phys. Rev. D* **2007**, *76*, 063007. [CrossRef]
86. Campanelli, L.; Cea, P.; Fogli, G.; Tedesco, L. Cosmic parallax in ellipsoidal universe. *Mod. Phys. Lett. A* **2011**, *26*, 1169–1181. [CrossRef]
87. Gruppuso, A. Complete statistical analysis for the quadrupole amplitude in an ellipsoidal universe. *Phys. Rev. D* **2007**, *76*, 083010. [CrossRef]
88. Cea, P. The ellipsoidal universe in the Planck satellite era. *Mon. Not. R. Astron. Soc.* **2014**, *441*, 1646–1661. [CrossRef]
89. Tedesco, L. Ellipsoidal Universe and Cosmic Shear. *Universe* **2024**, *10*, 363. [CrossRef]
90. Stuckey, W. The observable universe inside a black hole. *Am. J. Phys.* **1994**, *62*, 788–795. [CrossRef]
91. Seshavatharam, U. Physics of rotating and expanding black hole universe. *Prog. Phys.* **2010**, *2*, 7–14.
92. Popławski, N.J. Cosmology with torsion: An alternative to cosmic inflation. *Phys. Lett. B* **2010**, *694*, 181–185. [CrossRef]
93. Susskind, L. The world as a hologram. *J. Math. Phys.* **1995**, *36*, 6377–6396. [CrossRef]
94. Bak, D.; Rey, S.J. Holographic principle and string cosmology. *Class. Quantum Gravity* **2000**, *17*, L1. [CrossRef]
95. Bousso, R. The holographic principle. *Rev. Mod. Phys.* **2002**, *74*, 825. [CrossRef]
96. Myung, Y.S. Holographic principle and dark energy. *Phys. Lett. B* **2005**, *610*, 18–22. [CrossRef]
97. Hu, B.; Ling, Y. Interacting dark energy, holographic principle, and coincidence problem. *Phys. Rev. D* **2006**, *73*, 123510. [CrossRef]
98. Rinaldi, E.; Han, X.; Hassan, M.; Feng, Y.; Nori, F.; McGuigan, M.; Hanada, M. Matrix-Model Simulations Using Quantum Computing, Deep Learning, and Lattice Monte Carlo. *PRX Quantum* **2022**, *3*, 010324. [CrossRef]
99. Sivaram, C.; Arun, K. Holography, dark energy and entropy of large cosmic structures. *Astrophys. Space Sci.* **2013**, *348*, 217–219. [CrossRef]
100. Shor, O.; Benninger, F.; Khrennikov, A. Representation of the universe as a dendrogramic hologram endowed with relational interpretation. *Entropy* **2021**, *23*, 584. [CrossRef]
101. Edwards, M.R. Shell Universe: Reducing Cosmological Tensions with the Relativistic Ni Solutions. *Astronomy* **2024**, *3*, 220–239. [CrossRef]
102. Ashmore, L.E. Data from Twenty-Three FRB's Confirm the Universe Is Static and Not Expanding. *J. High Energy Phys. Gravit. Cosmol.* **2024**, *10*, 1152–1177. [CrossRef]
103. Capozziello, S.; Sarracino, G.; De Somma, G. A Critical Discussion on the Ho Tension. *Universe* **2024**, *10*, 140. [CrossRef]
104. Vagnozzi, S. New physics in light of the H 0 tension: An alternative view. *Phys. Rev. D* **2020**, *102*, 023518. [CrossRef]
105. Rameez, M.; Sarkar, S. Is there really a Hubble tension? *Class. Quantum Gravity* **2021**, *38*, 154005. [CrossRef]
106. Di Valentino, E.; Mena, O.; Pan, S.; Visinelli, L.; Yang, W.; Melchiorri, A.; Mota, D.F.; Riess, A.G.; Silk, J. In the realm of the Hubble tension—A review of solutions. *Class. Quantum Gravity* **2021**, *38*, 153001. [CrossRef]
107. Aloni, D.; Berlin, A.; Joseph, M.; Schmaltz, M.; Weiner, N. A step in understanding the Hubble tension. *Phys. Rev. D* **2022**, *105*, 123516. [CrossRef]

108. Davis, T.M.; Hinton, S.R.; Howlett, C.; Calcino, J. Can redshift errors bias measurements of the Hubble Constant? *Mon. Not. R. Astron. Soc.* **2019**, *490*, 2948–2957. [CrossRef]
109. Glazebrook, K.; Nanayakkara, T.; Schreiber, C.; Lagos, C.; Kawinwanichakij, L.; Jacobs, C.; Chittenden, H.; Brammer, G.; Kacprzak, G.G.; Labbe, I.; et al. A massive galaxy that formed its stars at z ≈ 11. *Nature* **2024**, *628*, 277–281. [CrossRef]